Electric Power Systems Research 92 (2012) 115–122

Contents lists available at SciVerse ScienceDirect

Electric Power Systems Research

journal homepage: www.elsevier.com/locate/epsr

Detailed three-phase circuit model for power transformers over wide frequency range based on design parameters

M. García-Gracia[a], M. Villén[a], M.A. Cova[a,*], N. El Halabi[a,b]

[a] Centre of Research for Energy Resources and Consumption (CIRCE)/Mariano Esquillor, 15/50018 Zaragoza, Spain
[b] Centro Universitario de la Defensa, AGM, 50090 Zaragoza, Spain

ARTICLE INFO

Article history:
Received 24 October 2011
Received in revised form 25 April 2012
Accepted 25 June 2012
Available online 20 July 2012

Keywords:
High frequency
Power transformers
Design parameters
Surge voltage
Lightning discharge

ABSTRACT

This paper presents a detailed three-phase transformer model, the elements of which are expressed analytically according to the physical layout and the design construction parameters of the power transformer. These expressions have been calculated theoretically and verified through finite elements simulations.

The proposed model allows to obtain the internal voltage distribution through the three-phase transformer in any type of operating condition, particularly when it is simulated in an electromagnetic time domain transient simulation tool, providing an external and internal characterization of the transformer in a frequency band that can appear in a power system (up to 1 MHz).

The obtained results have been compared with both lightning and low frequency tests measurements, showing a good agreement.

1. Introduction

Transformers are probably one of the most common components in a power system and also turn to be one of the most difficult to be properly modelled. Transformers are often exposed to a variety of high voltage transients. Lightning discharges, several types of faults, switching operations, and nonlinear loads, often cause high frequency oscillations and produce transient high voltage stresses at the transformer windings [1].

If a transformer is under a voltage transient, like lightning discharges or switching surges, it could reach undesirable operation points, near to its resonance frequency, which may cause the collapse of the transformer [2,3].

Power transformers are critical components of energy transmission and distribution processes. In view of increasing demand for reliable and high-quality energy supply, electrical utilities are more interested in avoiding transformer failures [4,5].

From the manufacturer point of view, the interest is to have a more accurate cost-effective design of the power transformer, especially in the internal insulation, having an exact knowledge about the internal behaviour of the transformer with its surroundings. Once an inter-turn fault occurs, high fault current flows through shorted turns, leading to a severe damage of the defective region in the winding [6]. Therefore, a good knowledge of transformers in disturbance conditions is needed. The variety of proposed models can be classified as [7]: black box models, physical models and hybrid models.

Black box models are dependent on the measured data from the terminals of the transformer. These models do not allow considering any internal fault. Its admittance matrix is calculated from measurements, and then each element of this matrix is approximated with an equivalent circuit. The method used for this modelling is powerful, but the admittance matrix measurement is difficult to be handled and have no useful information about the real phenomena inside the transformer [7–9]. The use of simple models like black box models may be justified by a lack of available information.

Physical models are based on Finite Element Method (FEM) or several Resistance, Inductance, Capacitance (RLC) elements, then the simulation run time is expensive and their usage by power network analysis is limited due to their numerous elements [10–13].

Hybrid models combine both previous models and are commonly used to increase the frequency limit range of simulations [14–16]. These models are constructed by combining the transformer detailed lumped parameter equivalent model and the Multi-conductor Transmission Line (MTL) model. The hybrid model parameters are calculated employing the detailed lumped equivalent model parameters and then, based on these parameters the MTL formulation is employed for partial discharge location. This

* Corresponding author. Tel.: +34 946 761000x5164.
E-mail address: cova@unizar.es (M.A. Cova).

0378-7796/$ – see front matter © 2012 Elsevier B.V. All rights reserved.
http://dx.doi.org/10.1016/j.epsr.2012.06.015

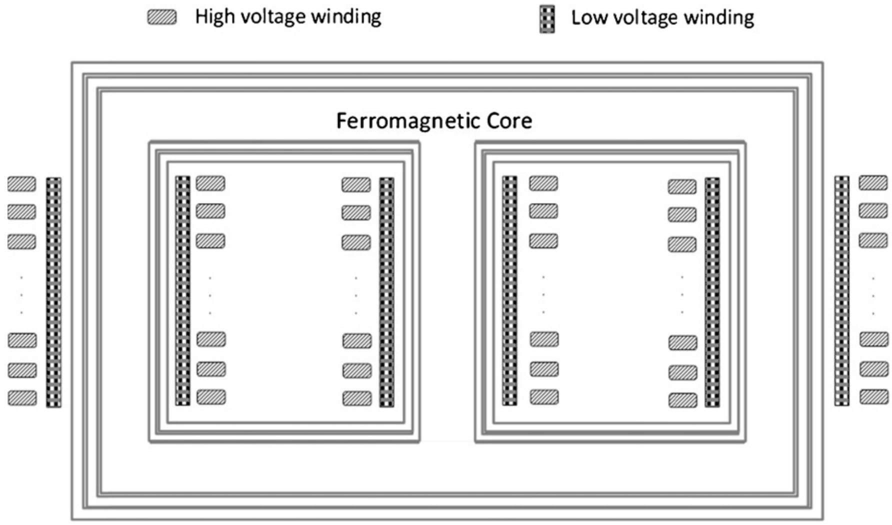

Fig. 1. Internal transformer composition.

combination is suggested to be able to model the transformer winding for a wide range of frequencies [17–22].

The aim of this paper is to create a hybrid model based on transformer design parameters through analytical formulas [23], so the parameter of this model does not require any costly and time-consuming measurements. The external and internal behaviour of the developed model has been compared with experimental tests. This model allows calculating accurately the voltage in any part inside the transformer and also to be simulated as black box in large power network simulations.

2. Distributed parameter circuit for transformer model

A discretized model of three-phase power transformers has been developed through electromagnetic transient program, to reproduce voltage distribution along its internal composition once an overvoltage discharge appears.

A blueprint of the internal composition of the power transformer, including the high and low voltage windings and the ferromagnetic core is shown in Fig. 1. This schematic helps to understand the real construction layout and the equivalent model configuration developed. Fig. 2 outlines the geometrical dimensions of three-phase power transformer used to evaluate the developed model.

The transformer is constructed by a laminated ferromagnetic core and HV and LV coils, wounded to a cylindrical column of core. In Fig. 1 each one of the three HV and LV windings are shown. They are composed of n discs, built each one of them by coil turns of conductive material and isolated by epoxy.

To create a power transformer model able to reproduce the internal behaviour, the transformer has been divided in n sections which correspond to the n discs of HV winding. The electromagnetic effects that each one of these divisions has with their surrounding are considered.

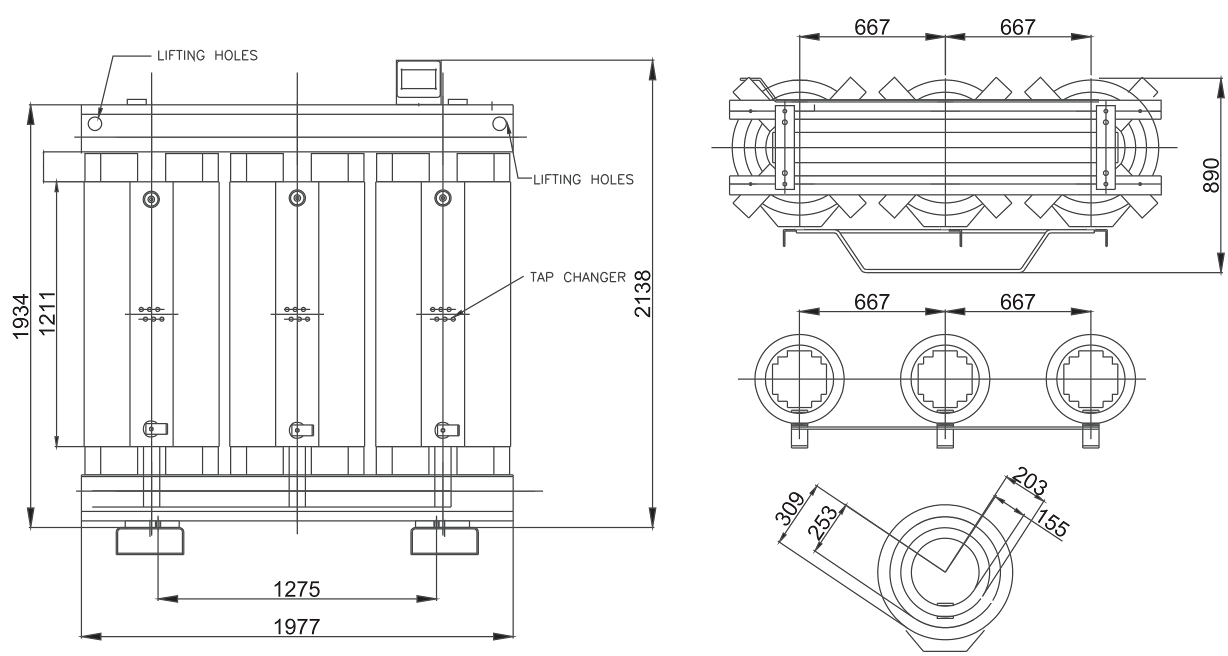

Fig. 2. Drawings of the power transformer modelled.

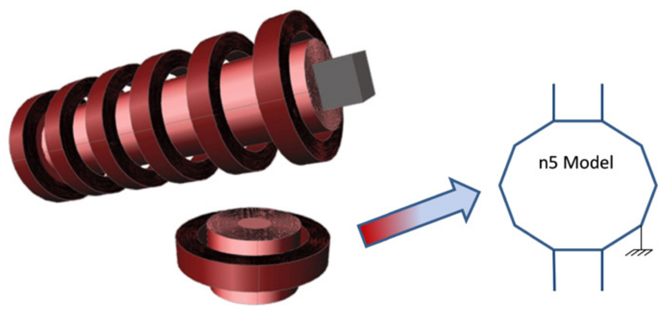

Fig. 3. Model representation by phase.

Fig. 3 shows the prior division, which includes a HV disc, an imaginary section of the LV winding and its corresponding ferromagnetic core section. The first and last HV discs of power transformer model also include the ferromagnetic core corresponding to the superior or inferior boundary, depending on the case. Each division is represented by a 5-port model called $n5$, with 5 connections; two toward its subsequent model, two toward its previous model and one connected to ground, giving place to a composition of n models $n5$ representing an entire phase of power transformer.

To build the complete model of the three phase transformer in PSCAD [27], n several number models $n5$ interconnected with each other have been represented, therefore each of the 3 columns that includes the transformer contain an entire phase (HV and LV windings), resulting in a model of $3n$ sub-elements $n5$.

Fig. 4(a) shows the global model of the power transformer as a set of sub models that contain the equivalent circuit of each section in which the transformer has been divided [26]. This division allows obtaining the internal voltages among the HV discs.

Each one of the n elements represents the electric behaviour of an internal section of the transformer and reproduces the electromagnetic phenomena that occur in each section bounded by a disc.

The model components reproduce the transformer behaviour during slow and fast transients and characterize the transformer at low frequency as well, retaining the classical equivalent circuit of power transformers, which is calculated from the short circuit and no load tests.

The detailed model of each $n5$ port is shown in Fig. 4(b). It consists of 23 electrical components that characterize this transformer in a frequency band from 0 to 1 MHz, covering the frequency spectrum that can appear in a power system due to transients. $R_{f\text{-LV}}$ and $R_{f\text{-HV}}$ denote the resistance at high frequencies in the low and high voltage winding respectively. $L_{\text{HV–LV}}$ and $L_{\text{LV–HV}}$ outlines the self and mutual inductive effect between the HV and LV windings and vice versa respectively. $C_{\text{HV-}g}$ denotes the capacitances effects between the first or last disc of HV winding with the ferromagnetic core. $C_{\text{LV-}g}$ denotes the capacitances effects between the LV winding and ferromagnetic core. $C_{T\text{-}T\ \text{LV}}$ and $C_{T\text{-}T\ \text{HV}}$ reproduce the capacitances effects between each one of the turns composing the HV and LV winding respectively. $C_{\text{HV-}D}$ denotes the capacitive effect between HV discs and $C_{\text{HV–LV}}$ represents the capacitive effect between HV and LV windings. Finally the grey dash line contains the classical equivalent circuit model of a power transformer.

3. Calculation methods for electric circuit parameters

All parameters of the developed model have been obtained from the physical layout and dimensions of the power transformer with some theoretical approaches. In order to validate the calculated capacitance values from design parameters, the same transformer has been simulated in two software tools, by finite element methods in 2D and 3D, depending on symmetry.

3.1. Capacitive effect between HV discs

The capacitive effect between HV discs could be approximated according the physical constructive design parameters shown in Fig. 5(a). Each disc of HV winding is composed of a set of concentric turns from a specific external radius $Rext_{\text{HV}}$ to an internal radius $Rint_{\text{HV}}$ with an exact separation d_{ins}.

Using the Gauss' law to evaluate the electric field, the capacitance between HV discs is given by the following expression:

$$C_{\text{HV-}D} = \frac{2\pi\varepsilon_0\varepsilon_r(Rext_{\text{HV}}^2 - Rint_{\text{HV}}^2)}{d_{\text{ins}}} \tag{1}$$

To calculate the existing capacitance between consecutive discs of HV winding through FEM, the following elements are considered: *Disc i*, *Disc i* + 1, insulation and surrounding air, as shown in Fig. 5(b).

Due to the symmetry of the model, the simulation has been done using the electrostatic calculation module of 2D finite element software [30]. In this module, at each mesh point, the value of electric potential V is obtained by solving (2).

$$-\varepsilon\nabla^2 \cdot V = \rho \tag{2}$$

where ε represents the electrical permittivity, V the scalar electrical potential and ρ the charge density.

In the 2D representation shown in Fig. 5(b), it is necessary to apply a potential difference between their discs to create the electric field needed to calculate the capacitance. Fixing a voltage condition on each disc surface; a high voltage value on surfaces that define *Disc i*, and a low voltage value for areas in the *Disc i* + 1.

Once the problem has been simulated, the capacitance value between HV discs is obtained from the estimated value of stored energy and voltage difference between discs, using the following equation:

$$C = \frac{2Energy\_stored}{\Delta V^2} \tag{3}$$

3.2. Capacitive effect between turnings of a HV discs

Considering that HV windings are composed of concentric turns with insulating material of electric relative permittivity ε_r between each lap, the cylindrical capacitor formulation can be used to calculate $C_{T\text{-}T}$. Furthermore, as all capacitances are in series, the total capacitance can be expressed as:

$$C_{T\text{-}T} = \left(\sum_{1}^{n} \frac{2\pi\varepsilon_0\varepsilon_r h_{\text{ins}}}{\ln(Rext_{\text{HV}} + \Delta r_{i+1})/(Rint_{\text{HV}} + \Delta r_i)}\right)^{-1} \tag{4}$$

where h_{ins} is the height of one disc, Δr the separation between each lap and n is the total turn number of each disc.

The parameter $C_{T\text{-}T}$ is also calculated using 2D FEM. In this case, the elements considered for the simulation are the turns i and $i+1$ associated to a *Disc j*, as shown in Fig. 6.

Once the proposed system is solved, the capacitance between turns i and $i+1$ is calculated using (3). As stated before, the total capacitance is determined considering that all the capacitances are in series.

3.3. Capacitive effect between ends HV disc and the ferromagnetic core

It is possible to use an approximation to estimate the capacitance value between the first or last disc included in the HV winding

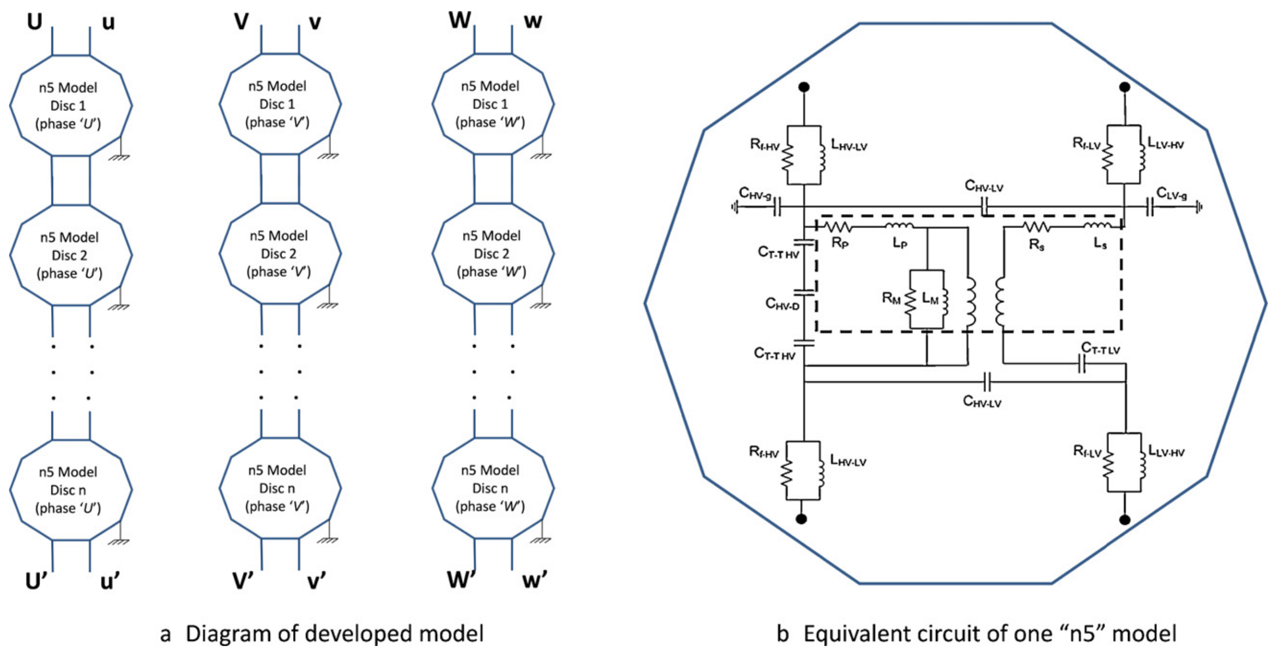

Fig. 4. Developed model of disc type power transformer.

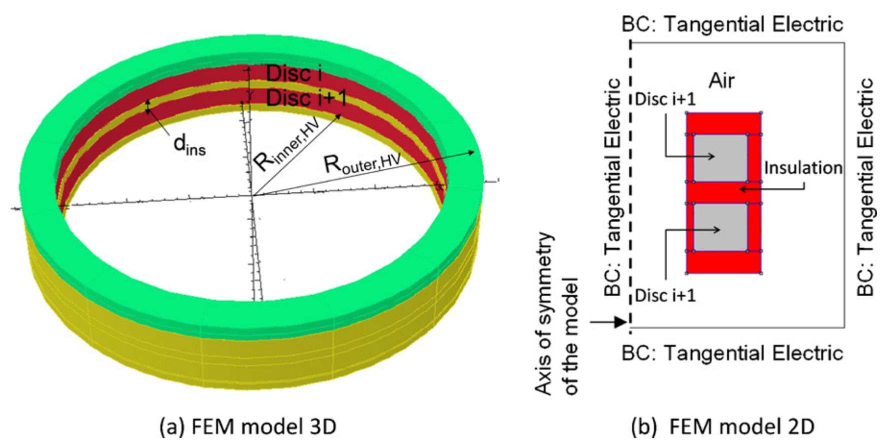

Fig. 5. FEM model of one disc included in HV winding.

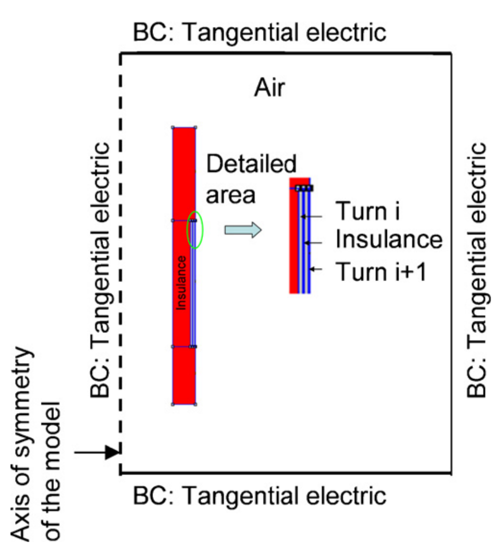

Fig. 6. Capacitive effect between HV discs turnings model description in FEM 2D.

respect to ferromagnetic core. Applying the Gauss' law the capacitance value $C_{\text{HV-}g}$ is obtained as follows:

$$C_{\text{HV-}g} = \varepsilon_0\varepsilon_r \frac{\int_{-Rext_{\text{HV}}}^{Rext_{\text{HV}}} \sqrt{(Rext_{\text{HV}}^2 - x^2)dx} - \int_{-Rint_{\text{HV}}}^{Rint_{\text{HV}}} \sqrt{(Rint_{\text{HV}}^2 - x^2)dx}}{d_{\text{core}}} \quad (5)$$

where d_{core} is the distance between ends HV disc and the transversal ferromagnetic core as shown in Fig. 7(a).

Fig. 7(b) shows the components considered to determine the capacitance between the ends of HV discs and ferromagnetic core by FEM. These components are: *Disc* # 1 or *n*, core, insulation, air and the border of the model with boundary condition.

Due to lack of symmetry, the simulation has been performed on the 3D finite element software OPERA [28], with Tosca Static simulation module [29]. In this module, as happened in the 2D module, the value of electric potential *V* at each mesh point is obtained by solving (2).

In the model shown in Fig. 7(b) the capacitance $C_{\text{HV-}g}$ can be calculated if voltage difference is applied between disc and core.

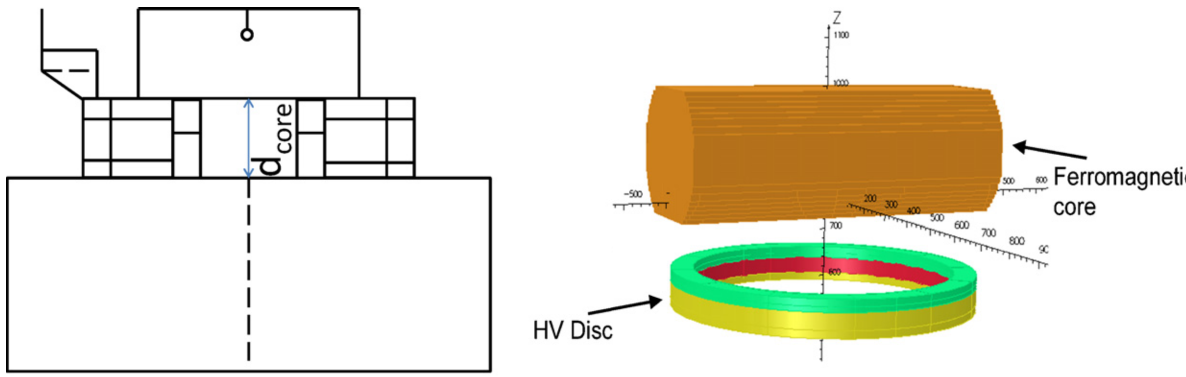

(a) Blueprint (b) FEM Model

Fig. 7. HV end discs and external ferromagnetic core.

Each disc surface and core has assigned a voltage condition, *high V* value for surfaces that define the disc and *low V* for core.

The insulating material surrounding the disc is an epoxy resin with a value of electric relative permittivity $\varepsilon_r = 4.1$; in FEM the mesh size considered is 7 mm.

3.4. Capacitive effect between HV and LV windings

The theoretical value is calculated using the cylindrical capacitor formulation and is expressed in terms of the power transformer constructive design parameters. This value represents the capacitance $C_{\mathrm{HV-LV}}$ in the disc placed at the middle of the HV winding (7). Due to the asymmetry of each HV disc with respect to the low voltage coil, the capacitance between HV and LV windings will not be constant among all discs. To take into account this asymmetry, the capacitance values for the rest of the disc are corrected using the Gauss distribution as follows:

$$C_{\mathrm{HV-LV}_i}(d) = ae^{\frac{-(d-n/2)^2}{2c^2}} + k \tag{6}$$

$$Cmed_{\mathrm{HV-LV}} = 2\pi\varepsilon_0 d_{\mathrm{ins}} \ln\left(\frac{Rint_{\mathrm{HV}}}{Rext_{\mathrm{LV}}}\right) \tag{7}$$

$$C_{\mathrm{HV-LV}}(n) = \mathrm{Cmin}_{\mathrm{HV-LV}} = ae^{\frac{-(n/2)^2}{2c^2}} + k \tag{8}$$

$$C_{\mathrm{HV-LV}}(n/2) = \mathrm{Cmax}_{\mathrm{HV-LV}} = a + k \tag{9}$$

$$C_{\mathrm{HV-LV}}(n/4) = Cmed_{\mathrm{HV-LV}} = ae^{\frac{-(n/4)^2}{2c^2}} + k \tag{10}$$

the constants a, c and k can be obtained from (8)–(10). These parameters just depend on the transformer physical layout.

The procedure used to calculate the capacitance $C_{\mathrm{HV-LV}}$ by FEM is analogous to the one used for the intern–turn capacitance calculation, with the difference that instead of two turns, a low voltage coil and a high voltage disc with its insulation are used. Fig. 8 shows the model associated with this simulation.

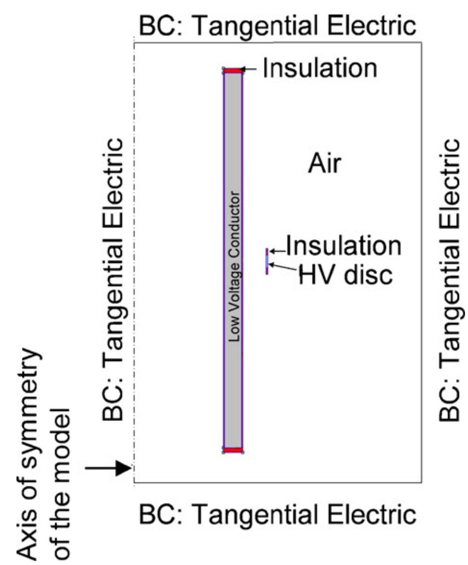

Fig. 8. Capacitive effect between HV discs turnings model description in FEM 2D.

3.5. Mutual inductance

To calculate a theoretical value of the inductive effect generated between discs of the HV windings a geometric approach of concentric windings is considered. This inductance is calculated using the following equation:

$$M_{i.i+1} = \frac{\mu_0 k' N_{\mathrm{HV}}^2 N_{\mathrm{LV}}^2 A h_{\mathrm{HV-LV}}}{h_{\mathrm{HV-LV}}} \tag{11}$$

where k' is the material permeability, N_{HV} and N_{LV} the turns numbers of HV and LV windings respectively, A is the cross-sectional area of the coil and $h_{\mathrm{HV-LV}}$ the height of each disc.

To obtain by FEM the inductance between two consecutive discs, a system composed of the core, the *Disc i* and *i* + 1 from HV winding and the surrounding air (Fig. 9) has been simulated on the 3D finite element software [28], with Tosca electromagnetic module.

Three different simulation scenarios are considered to calculate the inductance $M_{i,i+1}$. In the first one, a 1 A current flow through

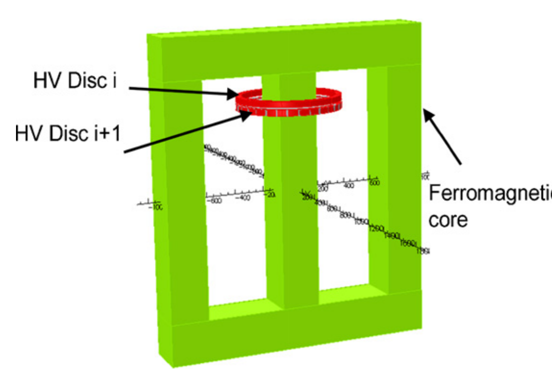

Fig. 9. 3D FEM model of two consecutive discs (HV winding).

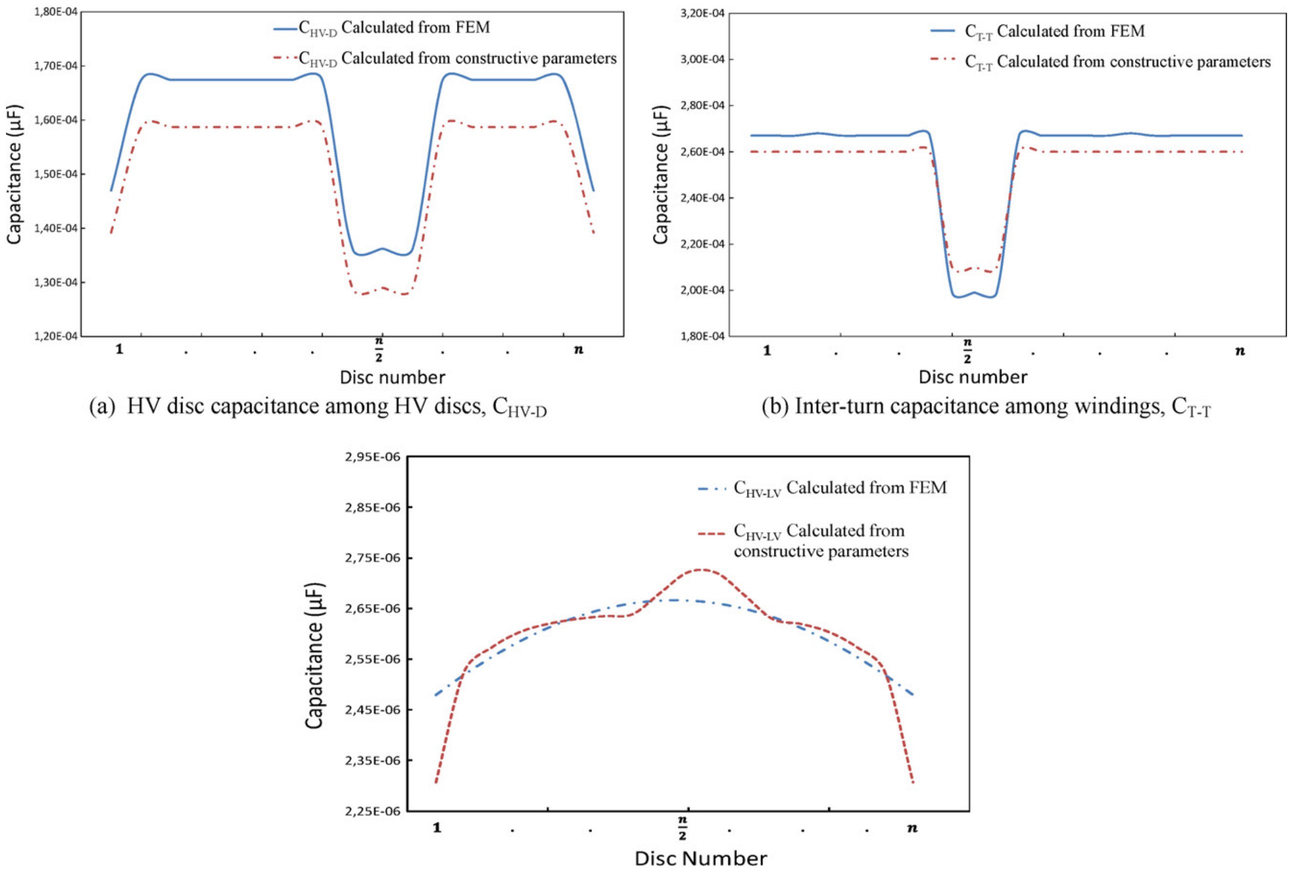

(a) HV disc capacitance among HV discs, $C_{HV\text{-}D}$

(b) Inter-turn capacitance among windings, $C_{T\text{-}T}$

(c) HV-LV disc capacitance distribution among windings, $C_{HV\text{-}LV}$

Fig. 10. Capacitance results comparison between theoretical approaches and FEM calculations.

Disc i while no current flows through *Disc i* + 1. In the second one, a 1 A current flow by the *Disc i* + 1 although no current flows through *Disc i*; and in the third one, a 1 A current flows over both discs at the same time.

Once all simulations are finished, the magnetic energy of the system is obtained in the three cases and the mutual inductance is calculated using the following equation:

$$M_{i,i+1} = W_{i,i+1} - W_{i,i} - W_{i+1,i+1} \tag{12}$$

where $W_{i,i+1}$ is the magnetic energy stored when a current is flowing through the discs, and $W_{i,i}$ and $W_{i+1,i+1}$ are the magnetic energy stored when a current flows through one of the discs.

4. Comparison of the calculation methods

The theoretical capacitance values derived in Section 3 are compared with the values calculated by FEM. These values, for each module *n*5, do not remain constant throughout the structure of the transformer, varying along each one of HV disc that conform the internal arrangement of the windings, the rest of parameters, inductances and resistances hold constant.

4.1. Results of capacitive effect between HV discs

Fig. 10(a) shows the values of the capacitances between HV discs ($C_{HV\text{-}D}$ element of *n*5 model), calculated through constructive physical layout and FEM estimation techniques.

The values obtained from FEM and theoretical approximation shows a good agreement, with and slight difference that remains constant among all discs.

4.2. Results of capacitive effect between turns of HV discs

In Fig. 10(b) the capacitance among turns of HV winding is shown. These values have been calculated through FEM estimation techniques and the theoretical equations derived from constructive design parameters, corresponding to $C_{T\text{-}T}$ element of *n*5 model.

In this case, values obtained from both theoretical and FEM techniques coincide well among all discs.

4.3. Results of capacitive effect between HV and LV windings

Fig. 10(c) shows the capacitances ($C_{HV\text{–}LV}$ element of *n*5 model) of the effect created between HV and LV windings, which have been calculated through FEM estimation techniques and design parameters.

The values comparison reveal that results obtained from both FEM and theoretical approximation using the Gauss distribution obtained in (6)–(10) shows a good agreement.

5. Comparison between simulation of the proposed model and experimental results

In order to verify the proposed model, jointly with the estimated parameters through FEM techniques, a lightning impulse has been simulated as indicates the protocols contemplated in IEC 60076-3 [31] standard to verify insulations on power transformers.

During the simulation, the maximum instantaneous voltage has been measured in each one of the internal disc of HV windings, and compared with the measures obtained at laboratory. The power

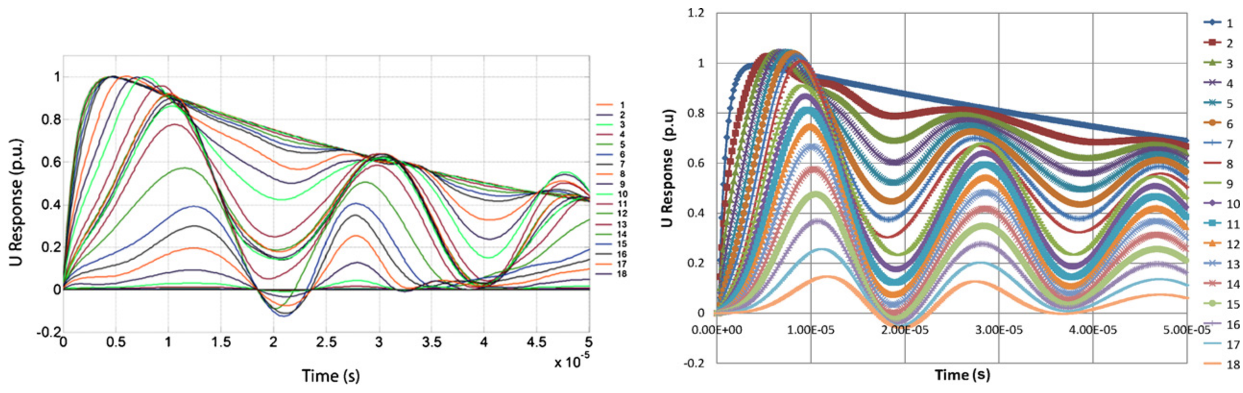

(a) Measurements (b) Simulations

Fig. 11. Instantaneous voltage distribution on transformer HV discs.

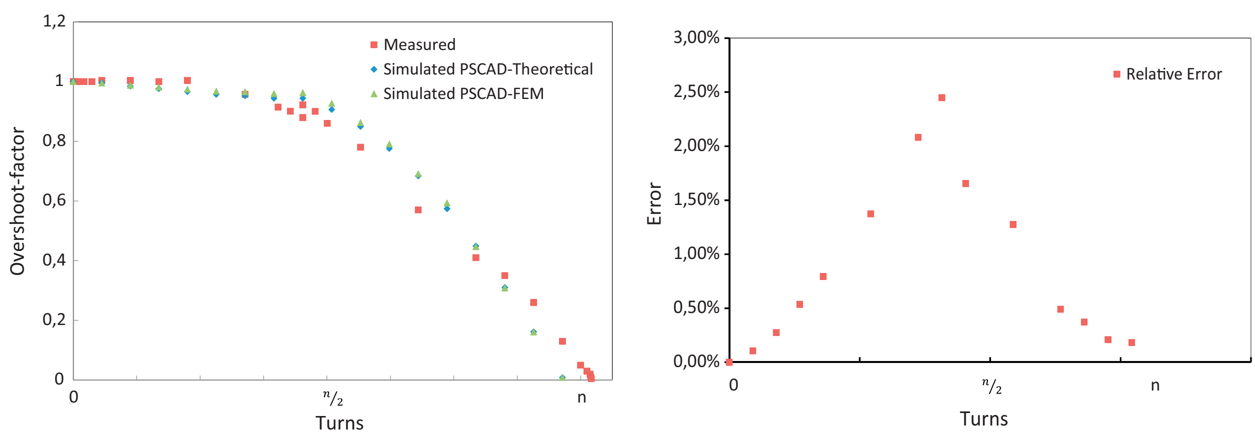

(a) Maximum voltage reached at HV winding coil (b) Relative error

Fig. 12. Comparison between theoretical approaches and FEM calculations of maximum voltages reached at HV discs.

transformer under study provides physical access to internal discs in order to record these measurements.

5.1. Power transformer test connection

The power transformer has been connected according to IEC 60076-3 standard. The connection is *Dy11* in which all terminals, except the phase where the lightning pulse is applied, are grounded.

5.2. Voltage distribution

In order to obtain the voltage distribution along the internal composition of the transformer, a wave impulse 1.2/50 μs on phase *U* is applied as described in standard IEC 60076-3.

Fig. 11(a) shows the instantaneous overshoot voltage distribution measured inside transformer during the impulse test. Fig. 11(b) shows same instantaneous overshoot voltage distribution, but in this case, results have been obtained from simulations.

It is noticed that measurements and simulation values have a similar behaviour between them with a slight time delay. From the comparison of the upslope, it is noticed a more accurate agreement of the developed model at high frequencies during the impulse test. The maximum amplitude of the first peak value of measurements is about 1.01 p.u. at 5 μs and the simulated amplitude is 1.03 at the same time. However, the measured amplitude of the maximum second peak value is about 0.64 p.u. at 30 μs and its simulated value is 0.8 p.u. at 28 μs.

Fig. 12(a) represents the instantaneous overshoot voltage reached in each one of the HV discs, these results come from two different PSCAD simulations of the developed circuit model; the first one with parameters obtained by FEM calculation method, and the second one with parameters calculated with theoretical approaches. These values are close to each other as well as the general shape, showing an error lower than 2.5% as shown in Fig. 12(b).

5.3. No load and short-circuit tests

In order to verify the behaviour of developed model at low frequencies, the no-load and short-circuit tests have been simulated. Table 1 provides a comparison of power losses during low

Table 1
Comparison of power losses at no load and short-circuit tests.

Test	Measured	Simulated (theoretical approaches)	Simulated (FEM parameters)
No load $(P_0/P_n) \times 100\%$	0.25%	0.23%	0.22%
Short-circuit $(P_{cc}/P_n) \times 100\%$	0.80%	0.78%	0.78%

frequency tests obtained from measurements and simulation results, with respect to transformer rated power.

The previous results confirm the accurate behaviour of proposed power transformer model at low frequencies.

6. Conclusions

A novel simulation model for three-phase power transformers has been developed, allowing studying the electromagnetic behaviour occurred inside the transformer at different operating conditions; especially against lightning surge discharges. The developed circuit model is determined using constructive design parameters of the transformer, allowing representation as an equivalent circuit composed of RLC elements interconnected in different parallel-series configurations.

FEM techniques have been used for both estimation of physical values of elements contained in the equivalent circuit developed and validation of those calculated from theoretical equation from the constructive and geometric design parameters.

The developed circuit model behaviour was validated through experimental tests performed. In these tests, the comparison is made of the maximum voltage overshoot in the internal discs, once a 1.2/50 μs lightning discharge is applied, according to the connection protocols and tests described in the IEC 60076-3 standard. The good agreement between measurements and simulations demonstrate the remarkable ability of the developed model to reproduce the real behaviour of power transformers at any operating frequency under 1 MHz.

The classic equivalent circuit of power transformers has been considered in the model, derived from no load and short-circuit tests made it by the manufacturer, the fact of include this parameters into the global model allow to represent a correct behaviour of power transformer at low frequency operation points, increasing the model frequency operation range from 0 up to 1 MHz.

The developed model can be used in electromagnetic transient programs to calculate fast transient responses of networks which contain transformers. This model can be applied not just to lightning surge analysis, but also to others applications such as propagation of high frequency partial discharge generated inside the transformer and post-lightning fault detection.

References

[1] Juan L. Velasquez-Contreras, Miguel A. Sanz-Bobi, Samuel Galceran Arellano, General asset management model in the context of an electric utility: application to power transformers, Electric Power Systems Research 81 (11) (2011) 2015–2037.

[2] P.M. Balma, R.C. Degeneff, H.R. Moore, L.B. Wagenaar, The effects of long term operation and system conditions on the dielectric capability and insulation coordination of large power transformers, IEEE Transactions on Power Delivery 14 (3) (1999) 960–971.

[3] Adam J. Thomas, Satish M. Mahajan, Capacitive weighting technique for estimating the 3D turn-level capacitance in a transformer winding, Electric Power Systems Research 81 (1) (2011) 117–122.

[4] A. Shintemirov, W.J. Tang, W.H. Tang, Q.H. Wu, Improved modelling of power transformer winding using bacterial swarming algorithm and frequency response analysis, Electric Power Systems Research 80 (9) (2010) 1111–1120.

[5] V. Behjat, A. Vahedi, Numerical modelling of transformers inter–turn faults and characterising the faulty transformer behaviour under various faults and operating conditions, IET Electric Power Applications 5 (5) (2011) 415–431.

[6] Luís M.R. Oliveira, A.J. Marques Cardoso, Sérgio M.A. Cruz, Power transformers winding fault diagnosis by the on-load exciting current extended Park's vector Approach, Electric Power Systems Research 81 (6) (2011) 1206–1214.

[7] E. Rahimpour, M. Bigdeli, Simplified transient model of transformer based on geometrical dimensions used in power network analysis and fault detection studies, in: International Conference on Power Engineering, Energy and Electrical Drives, 2009, pp. 375–380.

[8] S. Chimklai, J.R. Marti, Simplified three-phase transformer model for electromagnetic transient studies, IEEE Transactions on Power Delivery 10 (3) (1995) 1316–1324.

[9] T. Noda, H. Nakamoto, S. Yokoyama, Accurate modelling of core type distribution transformers for electromagnetic transient studies, IEEE Transactions on Power Delivery 17 (4) (2002) 969–976.

[10] Y. Shibuya, S. Fujita, N. Hosokawa, Analysis of very fast transient overvoltage in transformer winding, IEE Proceedings Generation, Transmission & Distribution 144 (5) (1997) 461–468.

[11] A.O. Soysal, A. Semlyen, Practical transfer function estimation and its application to wide frequency range representation of transformers, IEEE Transactions on Power Delivery 8 (3) (1993) 1627–1637.

[12] G. Liang, H. Sun, X. Zhang, X. Cui, Modeling of transformer windings under very fast transient overvoltages, IEEE Transactions on Electromagnetic Compatibility 48 (4) (2006) 621–627.

[13] T. Tran-Anh, P. Auriol, T. Tran-Quoc, High frequency power transformer modelling for power line communication applications, in: Power Systems Conference & Expo, 2006, pp. 1069–1074.

[14] G.B. Gharehpetian, H. Mohseni, K. Moller, Hybrid modelling of inhomogeneous transformer windings for very fast transient overvoltages studies, IEEE Transactions on Power Delivery 13 (1) (1998) 157–163.

[15] W.E. Archer, M.F. Deveney, R.L. Nagel, Non-linear transformer modeling and simulation, Proceedings of the IEEE Midwest Symposium on Circuits and Systems 1 (1994) 665–669.

[16] H. Gao, S. Wang, Y. Guo, N. Wei, Simulating calculation of transient voltage distribution for power transformer with software PSPICE, Proceedings of the Eighth International Conference on Electrical, Machines and Systems (ICEMS) 3 (2005) 1788–1790.

[17] H.K. Høidalen, B. Mork, F. Gonzalez, D. Ishchenko, N. Chiesa, Implementation and verification of the hybrid transformer model in ATPDraw, Electric Power Systems Research 79 (3) (2009) 454–459.

[18] M.S. Naderi, M. Vakilian, T.R. Blackburn, B.T. Phung, A. Nasiri, A hybrid transformer model for determination of partial discharge location in transformer winding, IEEE Transactions on Dielectrics and Electrical Insulation 14 (2) (2007) 436–443.

[19] B. Mork, F. Gonzalez, D. Ishchenko, D. Stuehm, J. Mitra, Hybrid transformer model for transient simulation—Part I: development and parameters, IEEE Transactions on Power Delivery 22 (1) (2007) 248–255.

[20] B. Mork, F. Gonzalez, D. Ishchenko, D. Stuehm, J. Mitra, Hybrid transformer model for transient simulation—Part II: laboratory measurements and benchmarking, IEEE Transactions on Power Delivery 22 (1) (2007) 256–262.

[21] A. Shintemirov, W.H. Tang, Q.H. Wu, A hybrid winding model of disc-type power transformers for frequency response analysis, IEEE Transactions on Power Delivery 24 (2) (2009) 730–739.

[22] G. Hoogendorp, M. Popov, L. van der Sluis, Application of hybrid modeling for calculating interturn voltages in transformer windings, IEEE Transactions on Power Delivery 24 (3) (2009) 1742–1744.

[23] F. de Leon, A. Semlyen, Efficient calculation of elementary parameters of transformers, IEEE Transactions on Power Delivery 7 (1) (1992) 376–383.

[26] A. Greenwood, Electrical Transients in Power Systems, second ed., Wiley-Interscience, USA, 1991.

[27] Manitoba HVDC Research Centre, PSCAD/EMTDC: electromagnetic transients program, 2005.

[28] Vector Fields, OPERA-3D, Opera finite element software.

[29] Vector Fields, OPERA-3D Cobham Technical Services Oxford OX5 1JE Reference Manual, Version 15, England, 2011.

[30] David Meeker, Finite Element Method Magnetics 4.2, Version 8, 1999.

[31] IEC 60076-3 Power transformers – insulation levels, dielectric tests and external clearances in air.